Journal of Biomolecular NMR, 3 (1993) 443–461
ESCOM

J-Bio NMR 136

^{1}H nuclear magnetic resonance determination of the membrane-bound conformation of senktide, a highly selective neurokinin B agonist

Beate Bersch[a,*], Patrice Koehl[b], Yoichi Nakatani[a], Guy Ourisson[a] and Alain Milon[c,**]

[a]*Laboratoire de Chimie Organique des Substances Naturelles, associé au CNRS, Centre de Neurochimie, Université Louis Pasteur, 5 rue Blaise Pascal, 67084 Strasbourg, France*
[b]*IBMC du CNRS, 15 rue Descartes, 67084 Strasbourg Cedex, France*
[c]*Laboratoire de Pharmacologie et de Toxicologie Fondamentales, CNRS, Université Paul Sabatier, 118 route de Narbonne, 31062 Toulouse, France*

Received 2 March 1993
Accepted 2 June 1993

Keywords: Transferred NOE; Distance geometry; Tachykinin; Active conformation; NK3 receptor

SUMMARY

Senktide is a highly specific and potent analog of neurokinin B, the natural ligand of the tachykinin receptor NK-3. The membrane-bound conformation of senktide, interacting with negatively charged membrane vesicles composed of perdeuterated phosphatidylcholine and phosphatidylglycerol (70:30), has been investigated using two-dimensional transferred nuclear Overhauser effect spectroscopy (TRNOESY). The occurrence of an N-methylated phenylalanine in the peptide's sequence induces a cis-trans-isomerisation of the corresponding peptide bond which is slow on the chemical-shift scale. NMR data indicate a much stronger membrane affinity of the trans isomer, allowing the determination of a highly resolved membrane-bound conformation using distance geometry and energy minimization. The membrane-bound backbone conformation of several residues is found to be close to a left-handed helix, certainly due to the presence of nonnatural residues (succinylated N-terminal, N-methyl-phenylalanine) as well as a glycine. The results are discussed in the context of a possible biological relevance of the membrane-bound conformation, in terms of the affinity and specificity of this neuropeptide.

INTRODUCTION

The tachykinins, a family of small bioactive peptides, are characterized by their common C-terminal sequence (Phe-X-Gly-Leu-Met-NH_2; X: Phe, Tyr, Val or Ile), and by their very similar biological profiles (for reviews see Maggio, 1988; Regoli et al., 1989; Guard and Watson, 1991). Tachykinins lower blood pressure and are involved in diverse processes such as the transmission

*Present address: Institut de Biologie Structurale, CNRS-CEA, 41 Avenue des Martyrs, 38027 Grenoble Cedex 1, France.
**To whom correspondence should be addressed.

0925-2738/$ 10.00 © 1993 ESCOM Science Publishers B.V.

of sensory information, nociception, smooth muscle contraction and inflammation. The amino acid sequences of the three best characterized tachykinins (substance P, neurokinin A and neurokinin B) are shown in Table 1.

Until now, at least three different tachykinin receptor subtypes have been identified by pharmacological, biochemical and molecular biology methods (Regoli et al., 1989; Guard and Watson, 1991; Nakanishi, 1991), but the existence of further subtypes cannot be excluded (Guard and Watson, 1991; Buck et al., 1991). Tachykinins are not highly specific for only one receptor subtype, but show some cross-reactivity with the other subtypes. The ligand specificity of the three receptor subtypes has been investigated in detail (Regoli et al., 1988,1989).

In recent years, potent and selective agonists of tachykinins have been developed, which were shown to be very useful for the pharmacological classification of tachykinin receptors in various tissues (Regoli et al., 1989). In most cases, these specific analogs have been obtained by introducing residues limiting the conformational freedom of the corresponding peptide. One possibility among others is the introduction of proline or N-methylated amino acids (Manavalan and Momany, 1980; Hrugy, 1982). From the analysis of binding data and from pharmacological investigations, it was shown that N-methylation of the phenylalanine in position 8 in the SP sequence, or of valine in position 7 in the NKB sequence, leads to very potent NK-3 agonists, possessing a much higher selectivity than neurokinin B, the natural ligand (Wormser et al., 1986; Drapeau et al., 1987; Lavielle et al., 1988; Loeuillet et al., 1989). Senktide (succinyl-[Asp^6, MePhe^8]SP(6–11)) has been shown to possess high affinity and selectivity for the NK-3 receptor and has been used to elucidate the NK-3 receptor distribution in various tissues (Laufer et al., 1986; Dam et al., 1990; Guard et al., 1990).

Its high selectivity and limited conformational freedom make senktide an excellent probe for the investigation of the biologically active conformations of tachykinins interacting with the NK-3 receptor. The characterization of the structural elements responsible for the specific receptor interaction and for the induction of the biological response is of great pharmacological interest.

It has been proposed that the interaction of neuropeptides with the membrane-embedded

TABLE 1
AMINO ACID SEQUENCE OF SUBSTANCE P, NEUROKININ A, NEUROKININ B AND SENKTIDE, A SPECIFIC NEUROKININ B ANALOG[a]

Peptide	Receptor	Sequence	Charge
Substance P	NK-1	Arg-Pro-Lys-Pro-Gln-Gln-Phe-Phe-Gly-Leu-Met-NH_2	+3
Neurokinin A	NK-2	His-Lys-Thr-Asp-Ser-Phe-Val-Gly-Leu-Met-NH_2	+1, +2
Neurokinin B	NK-3	Asp-Met-His-Asp-Phe-Phe-Val-Gly-Leu-Met-NH_2	0, −1
Senktide	NK-3	Succinyl-Asp-Phe-MePhe-Gly-Leu-Met-NH_2	−2

[a] Charges are given for physiological pH.

Abbreviations: SP, substance P; NKA, neurokinin A; NKB, neurokinin B; DMPC, 1,2-dimyristoyl-*sn*-glycero-3-phosphocholine; DMPC-d_{72}, perdeuterated 1,2-dimyristoyl-*sn*-glycero-3-phosphocholine; NOE, nuclear Overhauser effect; TRNOE, transferred nuclear Overhauser effect; TOCSY, total correlation spectroscopy; NOESY, nuclear Overhauser effect spectroscopy; ROESY, rotating frame nuclear Overhauser effect spectroscopy; TRNOESY, transferred nuclear Overhauser effect spectroscopy.

receptor molecules could involve intermediate steps, such as the accumulation, structuration and orientation of the peptide in the membrane prior to its binding to the receptor (Sargent and Schwyzer, 1986; Schwyzer, 1991 and references cited therein). For an optimal efficiency of the peptide–receptor interaction, the ligand must fit the spatial requirements of the receptor, which implies that interacting functional groups should be brought in close contact with each other. As has been pointed out by Schwyzer and co-workers, this 'optimal interaction' between peptide and receptor is less probable for the conformationally flexible peptide in solution than for the membrane-bound peptide, the latter being characterized by an enhanced local concentration, by an accelerated (two-dimensional) diffusion and by a limited conformational freedom in the amphiphilic and anisotropic environment represented by the lipid bilayer (Sargent and Schwyzer, 1986; Sargent et al., 1988). Therefore, the proposed multi-step mechanism involving the peptide–membrane interaction could explain that neuropeptides induce biological responses at very low bulk concentrations, often in the nanomolar range. Further support comes from numerous experimental results, correlating the biological activity of hormones or neurotransmitters with their membrane conformation (Wakamatsu et al., 1987; Jelicks et al., 1989; Behling and Jelinski, 1990; Milon et al., 1990), as well as from the observation of a pronounced membrane affinity of various neuropeptides, including substance P (Sargent et al., 1989; Seelig and Macdonald, 1989). Therefore, investigations of the structure of membrane-bound neuropeptides have been considered to be an important step towards the elucidation of the detailed mechanism of peptide–receptor interactions.

Nuclear magnetic resonance (NMR) spectroscopy represents a very powerful method for the structural investigation of biological macromolecules in solution (Wüthrich, 1986). However, the use of this technique becomes limited when the frequency of molecular reorientation $1/\tau_c$(τ_c = the correlation time of the molecule) in solution is low. In this case, the dipolar interaction is no longer averaged by molecular motion, and this induces a drastic line-broadening of the spectrum of the molecule and an accelerated spin-diffusion in nuclear Overhauser enhancement (NOE) measurements. These limiting conditions also hold for phospholipid vesicles, which are more adequate models of natural membranes than the much smaller micelles, but whose size (radii $\geq$ 20 nm) makes it impossible to study directly the bound ligand using high-resolution NMR.

The transferred NOE represents an indirect approach for obtaining structural information concerning a ligand bound to a macromolecule or to a phospholipid vesicle, even in the case where the overall correlation time of the ligand–membrane complex is too long to get any detailed information. This technique takes advantage of the rapid chemical exchange of the ligand between the bound and the free state, resulting in a transfer of bound-state information to the free ligand molecule, tumbling rapidly in solution (Clore and Gronenborn, 1983; Campbell and Sykes, 1991). TRNOE spectra are characterized by the occurrence of negative NOEs in the well-resolved spectrum of the free ligand, reflecting cross-relaxation pathways of the bound ligand.

In this work, we present the membrane-bound conformation of senktide, the selective neurokinin B analog, as derived from TRNOE investigations in the presence of perdeuterated phospholipid vesicles. From the TRNOE-derived distance constraints, the membrane-bound conformation was calculated using FILMAN, a new algorithm based on optimal filtering (Koehl et al., 1992). Using this approach, we were able to determine a family of very well resolved conformations, which could indicate the specific structural requirements of the NK-3 receptor.

MATERIALS AND METHODS

Senktide was purchased from Neosystem (Strasbourg, France) and was dissolved in 400 µl 95% H_2O/5% D_2O to a final concentration of 5 mM. The pH of the sample was adjusted to 4.8 by adding small volumes of 1N NaOH. No buffer was added in order to keep the ionic strength at a minimum. For NOE experiments performed in D_2O, the H_2O sample was lyophilized twice, the second time from D_2O to avoid isotopical dilution due to proton exchange. 400 µl D_2O (99.98%, Commissariat à l'Energie Atomique, Saclay, France) was added under argon atmosphere.

Perdeuterated 1,2-dimyristoyl-*sn*-glycero-3-phosphocholine (DMPC-d_{72}), 1,2-dimyristoyl-*sn*-glycero-3-phospho-*rac*-glycerol (DMPG-d_{64}) and 1,2-dimyristoyl-*sn*-glycero-3-phosphatidic acid (DMPA-d_{59}) were synthesized by a modification of the method described by Kingsley (Kingsley and Feigenson, 1979), as will be published elsewhere (Bersch et al., 1993). For the liposome preparation, DMPG-d_{64} was transformed to the free-acid form by adding small amounts of acidic ion– exchange resin (AG50W-X8, BIORAD) to a solution of DMPG-d_{64} in CH_2Cl_2/MeOH and filtration. Milligram amounts of phospholipids were mixed in the desired proportion (DMPC-d_{72}/DMPG-d_{64} 70:30, mol/mol) in dichloromethane solution containing 5 to 20% 2-propanol. After filtration (Millex-SR, 0.5 µm, Millipore Inc., USA), solvents were evaporated in a round-bottomed flask, leaving a thin lipid film, which was thoroughly dried under high vacuum overnight. Water (95% H_2O/5% D_2O) was added to give a final phospholipid concentration of 50 mM. Liposomes were formed by repeated vortex stirring at approximately 30 °C, which is above the phase-transition temperature ($T_c \leq 24$ °C for DMPC and for DMPG) (Wakamatsu et al., 1986). The pH was adjusted to 4.8. The suspensions were frozen (liquid nitrogen) and thawed three times to achieve a better homogeneity (Milon et al., 1990).

Preparation of TRNOE samples

Small volumes (10 µl) of the liposome suspension were added to the aqueous peptide solution until negative NOEs could be detected in one-dimensional difference spectra (300 ms mixing time), indicating the interaction of the peptide with the membrane. The phospholipid concentration was adjusted to obtain intraresidual TRNOEs of approximately −5% as measured for the Leu^{10} $C_\delta H_3$ to Leu^{10} $C_\beta H_2$. The final phospholipid concentration was 6.5 mM.

NMR experiments

All NMR experiments were carried out on a Bruker AMX 500 spectrometer, operating at a ^1H resonance frequency of 500 MHz. Data were processed on a Bruker X-32 workstation using the UXNMR program.

NOESY (Jeener et al., 1979) and TOCSY (Braunschweiler and Ernst, 1983; Bax and Davis, 1985b) experiments were performed both on the pure peptide in aqueous (H_2O) solution and in the presence of liposomes (TRNOESY). ROESY (Bothner-By et al., 1984; Bax and Davis, 1985a) spectra were acquired for the peptide in aqueous solution. For the unambiguous assignment of proton resonances, additional TOCSY, double-quantum filtered COSY (Rance et al., 1983; Shaka and Freeman, 1983) and two-dimensional double-quantum coherence spectroscopy (Braunschweiler et al., 1983) experiments were performed on the peptide in D_2O solution. These spectra were acquired with 64 scans, the latter in the absolute-value mode and with a 135° detection pulse (Mareci and Freeman, 1983). Unless otherwise indicated, all 2D NMR experi-

ments were acquired in the phase-sensitive mode with time-proportional phase incrementation (TPPI) of the initial pulse (Marion and Wüthrich, 1983), with 48 scans and a relaxation delay of 2 s. 512 t_1 increments and 2048 complex data points in t_2 were recorded for a spectral width of 5050 Hz in both dimensions. After zero-filling, the final size of the matrices was 1024 × 1024 real data points. Prior to Fourier transformation, the signal was multiplied in both dimensions by a 90° shifted square sine-bell window function. Usually a third- or fifth-order baseplane correction was performed in the two dimensions. Water suppression was achieved by selective irradiation of the water resonance during the relaxation delay (2 s) and during the NOESY mixing time. An additional TRNOESY experiment was performed without water presaturation, using a 'jump-and-return' read pulse (Plateau and Guéron, 1982). These data were used for the determination of distances from TRNOE intensities to check for any bleaching effect that presaturation may have on amide-to-α cross-peak intensities. For the TOCSY experiments an MLEV17 mixing scheme (Bax and Davis, 1985b) of either 10 or 90 ms with an 8-kHz spin-lock field strength was used. ROESY spectra were recorded with mixing times of 300 ms. The mixing was achieved by a continuous wave mixing with a field strength of 2.5 kHz. TRNOESY spectra were recorded with usual NOESY pulse sequences and with different mixing times (100, 200, 300 and 400 ms). From the spectra obtained with the different mixing times the linear buildup of the TRNOE was evaluated. Integral intensities were determined by the integration routine within the UXNMR program. Control NOESY spectra were acquired to evaluate the contribution of the free peptide to the TRNOESY spectra. They were acquired under identical conditions but in the absence of liposomes with a mixing time of 400 ms.

Deduction of distances from TRNOESY cross peaks

Internuclear distance information was obtained from TRNOE data by the evaluation of cross-peak volumes measured during the linear part of the buildup (two-spin approximation).

As in the NOE experiment, the ratio of two intermolecular distances can be related to the cross-peak volumes, measured in the linear proportion of the buildup curve (Clore and Gronenborn, 1983; Campbell and Sykes, 1991; Lippens et al., 1992; London et al., 1992):

$$\left(\frac{a_{ij}}{a_{kl}}\right) = \left(\frac{<\sigma_{ij}>}{<\sigma_{kl}>}\right) = \left(\frac{r_{ij}^{B}}{r_{kl}^{B}}\right)^{-6} \tag{1}$$

where a_{ij}, a_{kl} are the volumes of the cross peaks, $<\sigma_{ij}>$ and $<\sigma_{kl}>$ are the apparent cross-relaxation rates, and r_{ij}^{B}, r_{kl}^{B} are the internuclear distances of the bound state.

To obtain distance constraints, two different strategies were used simultaneously: because of the good resolution of the cross peaks in the TRNOESY spectrum, we integrated several cross peaks corresponding to backbone–backbone TRNOEs. From these, distances were estimated according to Eq. 1 (see below). For all the other cross peaks, upper bounds for the interproton distances were determined according to their relative intensities. They were attributed to four categories, weak (w), medium (m), strong (s), and very strong (vs), by counting the number of contour levels for each peak.

Cross-peak integration was performed on a TRNOESY spectrum acquired with a 'jump-and-return' read pulse (Plateau and Guéron, 1982). The reference distance was defined as follows: the integrals of all the $d_{N,\alpha}(i,i+1)$ cross peaks were compared. Setting the most intense cross peak to

a distance of 2.2 Å, we found that the weakest cross peak corresponded to a distance of 3.6 Å. These are, in fact, the upper and lower bounds for the chosen distance (Billeter et al., 1982; Saulitis and Liepins, 1990). TRNOE intensities were corrected for the contribution of more than two spins by dividing the cross-peak intensities by a normalization factor $(2N_aN_b)/(N_a + N_b)$, where N_a and N_b correspond to the number of protons under the cross peaks a and b, respectively (Macura and Ernst, 1980; Williamson and Neuhaus, 1987).

Calculation of the three-dimensional structures

As the peptide exchanges very rapidly between the free and the bound state, only the TRNOE-derived distances are suited to calculate the membrane-bound structure of senktide. From the TRNOE-derived distances, conformations were calculated with a new method, working in the dihedral-angle space. The strategy, implemeabnted in the program FILMAN, is based on nonlinear Kalman filtering (Koehl et al., 1992). With this procedure, the dihedral angles and their matrix of covariances are refined. In an initial covariance matrix, the range in which each angle is expected is defined, whereas the final covariance matrix provides estimates of errors on the dihedral angles according to the quality of the constraints.

FILMAN uses either estimated distances or distance ranges as input data. The former are entered with a variance (in $Å^2$) to take an estimate of distance error into account. To correct for an eventual contribution of the free peptide and errors due to imperfect peak integration, the variances used were 0.2 $Å^2$ for distances obtained from integrated TRNOESY cross peaks (corresponding to an evaluated distance error of 0.45 Å). In the case of the backbone N-methyl protons, the variance was set to 0.3 $Å^2$. As protons belonging to the side chains can be expected to have different correlation times cross peaks involving these protons were used only to define upper bounds of distance constraints (see below). The distance ranges include all distances from the sum of the two van der Waals radii to the upper bound, defined from the relative TRNOESY cross-peak intensities. The upper bounds were set as follows: 2.8 Å (vs), 3.2 Å (s), 4.0 Å (m) and 5.0 Å (w). Upper distance bounds of 5.0 Å (m) and 6.0 Å (w) were used for side-chain protons (γ, δ and aromatic side chains) to correct for a higher mobility of the interproton vector. For the FILMAN run using a limited set of constraints (Table 4), a possible distance error of 0.45 Å (or 0.2 Å) was given in the calculations for distances larger (or smaller) than 2.5 Å. Stereospecific assignments of aliphatic protons and of the glycine α-protons were not available in the first stage of refinement, thus the longer distances were used for the two protons. In the course of the structure refinement, stereospecific assignment of glycine α-protons could be deduced from the structure. For the aromatic side-chain protons, the distance constraints were referred to the δ- and ζ-carbon atoms (Wüthrich et al., 1983). Distances including methyl protons were also referred to their carbon atom (side chains) or to a pseudo-atom, located in the center of the three methyl protons (backbone N-methyl) (Wüthrich et al., 1983).

A starting set of 300 randomly created initial dihedral-angle files was used in the calculations. The initial standard deviation for each angle was set to 60° and all peptide bonds were maintained in the trans conformation by setting the ω angle to 180°. It was shown from NMR data that all the peptide bonds in the bound state were in the transconfiguration (no $C_\alpha H(i)$–$C_\alpha H(i + 1)$ cross peaks). The quality of the resulting structures was evaluated by the following parameters: the average distance error, the maximal distance error and the number of violations of van der Waals contacts. The average distance error is defined as follows:

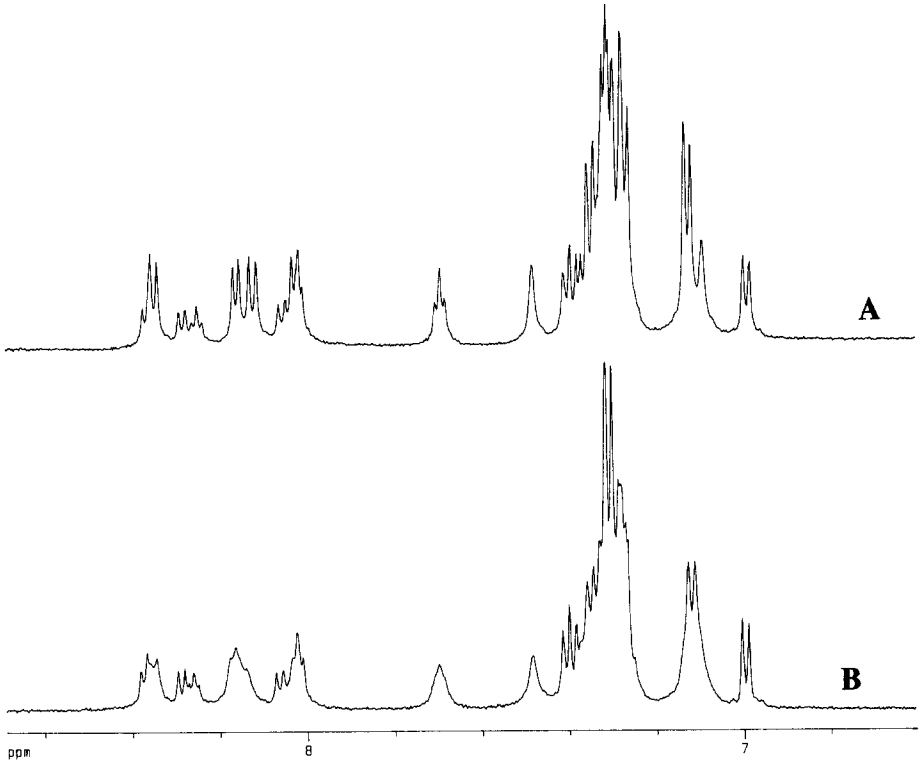

Fig. 1. One-dimension ^{1}H-spectra of senktide acquired in H_2O, showing the extension corresponding to the amide and aromatic protons (pH = 4.8, t = 30 °C). The spectra result from a mixture of cis (minor) and trans (major) isomers. (A) Spectrum in aqueous solution. (B) Spectrum in the presence of liposomes. The sample composition is as described in the experimental part; water suppression was achieved by presaturation during the relaxation delay (2 s).

$$\text{err.} = \frac{1}{N} \sum_{i=1}^{N} | d_{set}(i) - d_{model}(i) | \tag{2}$$

where N is the number of constraints and d_{set} and d_{model} correspond to the distance from the constraint set and to the distance calculated from the FILMAN conformation, respectively. The r.m.s.d value has been calculated as described by McLachlan; it is given by (McLachlan, 1979):

$$\text{r.m.s.d} = \left(\frac{1}{N} \sum_{i=1}^{N} (r(i) - r'(i))^2 \right)^{1/2} \tag{3}$$

where r(i) and r′(i) are the atomic coordinates corresponding to the two structures, and N the number of atoms being compared.

NOE back-calculations have been used in order to discriminate between three structural families consistent with one set of distance constraints, as will be discussed later. The principle consists of building a theoretical relaxation matrix from the coordinates of each proton in the molecule (Banks et al., 1989). These calculations were performed using PROTNOE, a program developed by P. Koehl. In our simulations we used a correlation time of 1 ns for all vectors in combination with a mixing time of 100 ms to correct for the rapid exchange of the peptide between a bound

($\tau_c \approx 10^{-7}\ s^{-1}$) and a free state ($\tau_c \approx 10^{-10}\ s^{-1}$) (Bersch et al., unpublished results). All these calculations were performed on an IBM RS6000 computer.

The calculated structures were visualized on an Evans and Sutherland PS 390 graphics station. Additional energy minimization was carried out using the SYBYL program (version 5.5) running on a SUN Sparcstation 2. In these calculations, the TRIPOS force field was used and the charges were set according to Gasteiger and Marsili (Gasteiger and Marsili, 1980).

RESULTS

^{1}H assignments

Although the peptide was shown to be chemically pure by HPLC and mass spectroscopy, the ^{1}H-spectrum of senktide in aqueous solution showed two distinct sets of resonance lines, with relative intensities of approximately 3:1 (see Fig. 1). The coexistence of the two ^{1}H-spectra was found to be independent of the solvent, the peptide concentration and the pH, but the intensity ratio was different in DMSO or methanol (data not shown). From a ROESY experiment these findings could be interpreted as the coexistence of two isomers, differing in the conformation of the peptide bond preceding the N-methylated phenylalanine (MePhe^8). A ROE between the Phe^7 $C_\alpha H$ and the MePhe^8 $C_\alpha H$ of the minor isomer showed that the peptide bond between the two residues is in a cis conformation (Wüthrich, 1986). For the major isomer this peptide bond was in the trans conformation, as illustrated by the ROE from Phe^7 $C_\alpha H$ to MePhe^8 $C_N H_3$.

^{1}H assignments of the two isomers were obtained from TOCSY experiments with different

TABLE 2
^{1}H ASSIGNMENTS OF THE TWO SENKTIDE ISOMERS IN H_2O [a]

Amino acid	H_N	$C_\alpha H$	$C_\beta H$	$C_\gamma H$	Other
Trans isomer					
Asp^6	8.02	4.52	2.48	–	–
Phe^7	8.14	4.89	2.92, 3.05	–	C_δ: 7.28; $C_\varepsilon H$: 7.35
MePhe^8	–	4.92	3.03, 3.29	–	$C_N H_3$: 2.79; $C_\delta H$: 7.12; $C_\varepsilon H$: 7.3
Gly^9	7.70	3.82, 3.95	–	–	–
Leu^{10}	8.17	4.39	1.68, 1.79	1.68	$C_\delta H_3$: 0.93, 0.98
Met^{11}	8.37	4.50	2.02, 2.13	2.53, 2.62	$C_\varepsilon H_3$: 2.08; NH_2 (C-terminal): 7.48 (cis), 7.10 (trans)
Cis isomer					
Asp^6	8.01	4.45	2.33, 2.48	–	–
Phe^7	8.06	4.62	1.79, 2.59	–	$C_\delta H$: 6.99; $C_\varepsilon H$: 7.32
MePhe^8	–	5.11	2.84, 3.34	–	$C_N H_3$: 2.96; $C_\delta H$: 7.3
Gly^9	8.26	3.95, 4.01	–	–	–
Leu^{10}	8.36	4.34	1.64	1.64	$C_\delta H_3$: 0.89, 0.93
Met^{11}	8.29	4.46	2.04, 2.14	2.54, 2.63	$C_\varepsilon H_3$: 2.10; NH_2(C-terminal): 7.42 (cis), 7.14 (trans)

[a] Succinyl protons could not be identified (see text). The $C_\zeta H$ protons of the two phenylalanines were not identified but might be superposed with the $C_\varepsilon H$ resonance lines. Cis and trans amide protons of the C-terminus are defined in relation to C_α. pH = 4.8, t = 30 °C. Gly^9 HA trans: 3.82 = pro*R*, 3.95 = pro*S*.

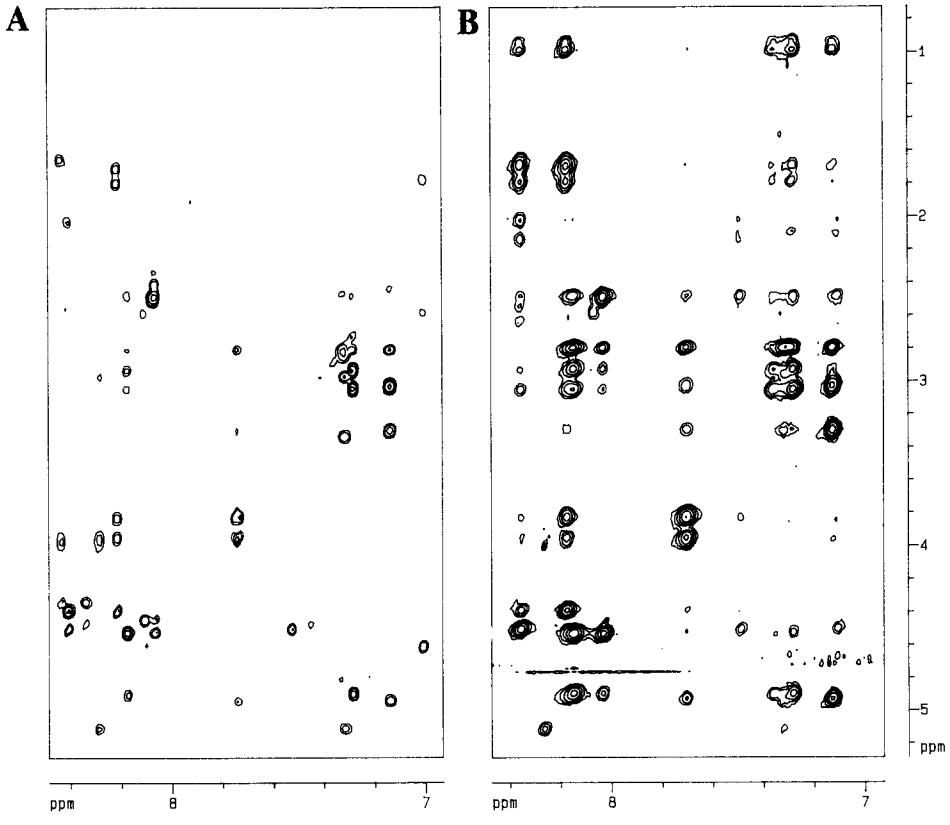

Fig. 2. The amide/aromatic–to–aliphatic cross-peak regions extracted from two-dimensional spectra of senktide in H_2O (pH = 4.8, t = 30 °C. (A) ROESY spectrum of senktide in H_2O. (B) TRNOESY spectrum of senktide (5 mM) in H_2O in the presence of liposomes (DMPC-d_{72}/DMPG-d_{64} 70:30 mol/mol; 6.5 mM). Solvent suppression was achieved by presaturation of the water resonance during the relaxation delay (2 s.).

mixing times. TOCSY experiments in D_2O were used to identify protons close to the water resonance. The assignments are shown in Table 2. The resonances of the succinyl protons of the two isomers could not be identified. Their chemical shift is close to the Asp^6 $C_\beta H_2$ protons and they did not give rise to any resolved cross peak in the TOCSY or DQF-COSY spectra; a double-quantum coherence spectroscopy experiment was performed, but again the succinyl protons were not resolved.

NMR experiments in aqueous solution

The ROESY spectrum (Fig. 2a) of senktide in aqueous solution only showed intraresidual and sequential connectivities, indicating that senktide does not occur in a single preferred conformation in aqueous solution. A similar behavior has been found for substance P (Chassaing et al., 1986).

In the NOESY spectrum (τ_m = 400 ms), only few and very weak positive cross peaks were identified (data not shown). Their intensity was estimated to be weak enough for neglecting the cross-relaxation of the free peptide in the interpretation of TRNOESY spectra. In addition,

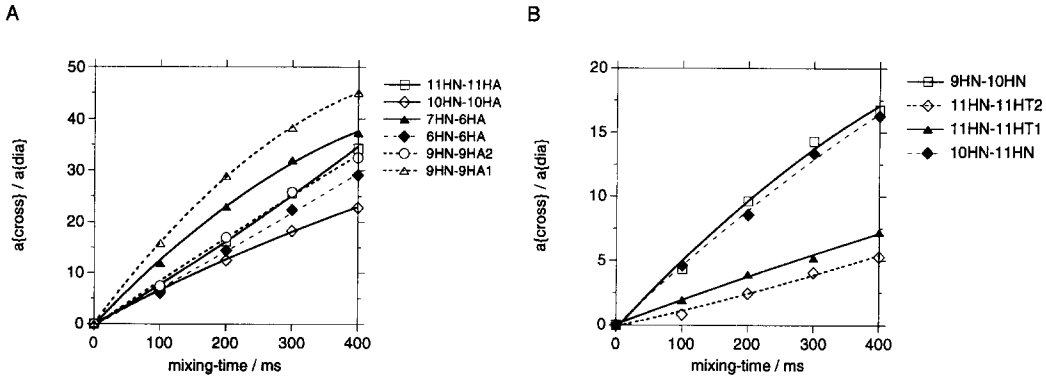

Fig. 3. Time dependence of transferred NOEs for mixing times of 100, 200, 300 and 400 ms. In order to correct for relaxation during the mixing time, cross-peak–to–diagonal-peak ratios have been calculated. The linear dependence of these ratios indicates the absence of a spin-diffusion artifact.

negative cross peaks were observed between corresponding resonances of the two isomers. They indicate the chemical exchange between the cis and the trans isomer.

NMR experiments in the presence of liposomes

Upon the addition of liposomes (70% DMPC-d_{72}, 30% DMPG-d_{64}, 6.5 mM), the resonances of the trans isomer showed a pronounced line broadening, indicating its interaction with the membrane. Interestingly, the lines corresponding to the cis-isomer did not show the same effect (Fig. 1). The same observations were made using liposomes formed with DMPA-d_{59} instead of DMPG-d_{64} (data not shown). The chemical-shift values of the resonance lines did not change when adding liposomes, as revealed by a TOCSY experiment (90 ms mixing time).

In the TRNOESY experiment, a high number of negative cross peaks demonstrated the interaction of senktide with the membrane (Fig. 2b). The appearance of amide–to–amide and medium-range cross peaks was in favor of a well-defined conformation of membrane-bound senktide. The identification of the negative cross peaks revealed that most of them were due to TRNOE effects between protons of the trans isomer of senktide. Only a few negative cross peaks appeared between resonances of the cis isomer. These were all intraresidual and did not give any information about a possible membrane-bound structure.

TRNOE buildup curves were obtained for various proton pairs, including amide–to–amide, amide–to–alpha and amide–to–side-chain cross peaks. Cross-peak volumes were obtained for different TRNOESY experiments with mixing times of 100, 200, 300 and 400 ms. These data were then corrected for relaxation effects during the mixing time by normalization with the average volume of diagonal peaks of amide protons. We observed a linear dependence on mixing time up to 300 ms, showing that spin-diffusion effects were negligible in our experimental conditions (Fig. 3). On the whole 99 TRNOEs were defined, including 37 backbone and sequential (i,i + 1) TRNOEs as well as 24 short- and medium-range (i,i + k; $k \geq 2$) distance constraints. Figure 4 summarizes several typical sequential, short- and medium-range connectivities. Because of the good resolution of the TRNOESY spectrum, 19 backbone–to–backbone cross peaks were integrated and the corresponding distances were determined as described in the experimental part

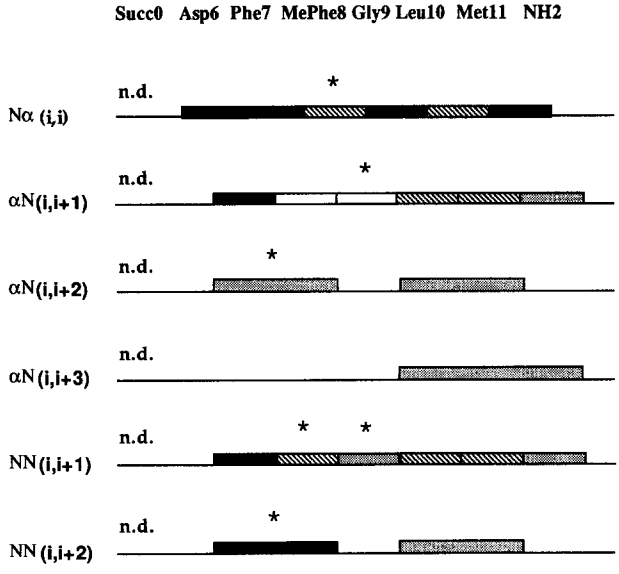

Fig. 4. Summary of sequential and medium-range TRNOEs detected for the membrane-bound senktide trans isomer. Black bars indicate strong, hatched bars medium, and dotted bars weak TRNOEs. White bars indicate TRNOEs whose intensity could not be measured due to overlap of several cross peaks. Asterisks correspond to TRNOEs involving the Phe^8 C_NH_3.

(Table 4). In the assignment of TRNOEs one problem arose due to the superposition of the methylene protons of $Succ^0$ and the β-protons of residue Asp^6. At this resonance frequency, several TRNOEs could be detected, including medium-range TRNOEs with the C-terminal amide protons. Therefore, FILMAN calculations were performed with different possible assignments.

Calculation of the three-dimensional structure

In a first set of calculations, the 99 TRNOE-derived distances or upper distance bounds were used as FILMAN input data to calculate the membrane-bound conformation of the trans isomer (the full set of constraints is available as supplementary material). In this set, the ambiguous TRNOEs were assigned to the Asp^6 $C_\beta H_2$. Out of the 9000 resulting structures obtained after refinement of the 300 initial random structures, the 10 best conformations found to be consistent with our input data were retained. The average distance error for constraints involving backbone atoms varied from 0.19 to 0.22, while the number of remaining van der Waals violations in the refined structures varied between 15 and 35. None of these violations were found to introduce severe clashes in the structures. It should be mentioned that such violations are difficult to avoid in a calculation based on a geometrical approach, but can be removed easily with an energy minimization procedure. The average rms calculated over the backbone atoms of the 10 selected structures is 0.29 Å. However, the maximum distance violations in this run (up to 0.8 Å) were not fully satisfactory. They appeared to be due mainly to proximities detected between the first two residues: Asp^6 HA–Phe^7 HN = 2.2 Å; Asp^6 HN–Phe^7 HA = 3.3 Å; $MePhe^8$ CH_3–Phe^7 HN = 2.7 Å.

An amount of 99 TRNOEs for a 6-residue peptide (not considering the succinyl chain) corresponds to approximately 16 constraints per residue. However, most of these constraints are redundant or noninformative. To illustrate this effect and to determine which constraints were really determining the final stucture, we selected a limited group of 30 constraints (see Table 4). A second set of FILMAN runs was performed with these input data, using the same 300 initial structures. Again the 10 best conformations selected by the program were retained. They were found to have similar main-chain conformations as the 10 best structures obtained with the complete data set (see Table 3). In these structures, of course, side chains were less refined (results not shown). Distance violations were found to be very similar in the 10 structures, and are shown in Table 4 in the case of the 'best' structure selected in this second set of calculations. Again the same three distances were violated while the remaining constraints were remarkably well satisfied, with an average distance error of 0.1 Å (0.26 SD) and a maximum distance error of 0.25 Å. It can be seen that these three violated distances are not compatible with one single conformation; the Asp^6 HA–Phe^7 HN = 2.2 Å distance imposes a ψ^1 such that the other distances cannot be satisfied. The distance involving MePhe^8 CH_3 is a special case where a systematic error in the calculation of the distance cannot be excluded. We conclude therefore that several conformations must coexist at the level of the N-terminus (angles ϕ^1, ψ^1 and ϕ^2) while the rest of the structure is very well defined.

Energy minimization of one of the conformations was performed: the main-chain conformation is highly similar and only minor reorientations of the Leu^{10} and the MePhe^8 side chains were seen. The total energy of the starting compound was 296 kcal/mol with a van der Waals energy of 145 kcal/mol. At the end of the energy minimization process, the total energy was found to be −3 kcal/mol. Figure 5 shows a superposition of the FILMAN conformation before and after

TABLE 3
AVERAGE FILMAN VALUES FOR THE Φ AND Ψ BACKBONE TORSION ANGLES AND THEIR STANDARD DEVIATIONS

	ϕ angle (degrees)			ψ angle (degrees)		
Residue	Average value[a]	STD1[b]	STD2[c]	Average value	STD1[b]	STD2[c]
Succ^0	[d]	–	–	[d]	–	
Asp^6	147 (135)	17 (2)	21 (15)	51 (70)	11 (1)	15 (7)
Phe^7	41 (38)	8 (1)	19 (17)	74 (78)	4 (1)	11 (11)
MePhe^8	45 (55)	6 (5)	10 (11)	15 (10)	4 (4)	18 (20)
Gly^9	60 (54)	6 (2)	16 (19)	23 (28)	6 (2)	19 (22)
Leu^{10}	−49 (−45)	2 (1)	25 (14)	−33 (−21)	3 (3)	17 (32)
Met^{11}	153 (128)	6 (2)	31 (22)	[d]	–	–

[a] The values in parentheses correspond to the 10 best structures refined with the limited set of constraints (Table 4), while the other values correspond to the 10 best structures obtained with the full set of constraints (see Results).
[b] Standard deviation taken over the refined structures. These values describe the size of the family of structures which were compatible with the data and are dependent on the number of structures selected.
[c] Standard deviation provided by FILMAN in the least-square sense. STD2 provides a more realistic estimation of the precision of the structure.
[d] Mixture of conformations.

energy minimization. This result shows that a table conformation without van der Waals contacts can exist within the same family of structures.

DISCUSSION

In the presence of liposomes, only the spectrum of the trans isomer of senktide showed the characteristic line broadening and the negative NOEs indicating its membrane interaction. This is in favor of a different membrane affinity of the two isomers, which should be due to a different

TABLE 4
SIGNIFICANT SET OF 30 TRNOE-DERIVED CONSTRAINTS AND CORRESPONDING DISTANCE VIOLATIONS IN ONE REFINED STRUCTURE OF SENKTIDE

Atom 1	Atom 2	Distance constraint (Å)	Distance in the structure (Å)	Distance error/SD[a]
Asp^6 HN	Asp^6 HA	2.51	2.54	0.13
Phe^7 HN	Asp^6 HN	2.42	2.34	0.15
Phe^7 HN	Asp^6 HA	2.20	2.49	1.29
Phe^7 HN	Phe^7 HA	2.14	2.27	0.60
Phe^7 HA	Asp^6 HN	3.31	4.15	1.87
MePhe^8 CH_3	Asp^6 HN	3.87	3.62	0.46
MePhe^8 CH_3	Phe^7 HN	2.70	3.33	1.15
Gly^9 HN	MePhe^8 CH_3	3.35	3.26	0.16
Gly^9 HN	MePhe^8 HA	3.35	3.21	0.31
Gly^9 HN	Gly^9 HA	2.20	2.25	0.23
Gly^9 HN	Gly^9 HA2	2.58	2.76	0.39
Leu^{10} HN	Gly^9 HN	2.75	2.70	0.10
Leu^{10} HN	Gly^9 HA2	3.52	3.52	0.01
Leu^{10} HN	Gly^9 HA	2.83	2.99	0.35
Leu^{10} HN	Leu^{10} HA	2.62	2.71	0.20
Met^{11} HN	Gly^9 HN	4.27	4.39	0.26
Met^{11} HN	Leu^{10} HN	2.94	2.81	0.30
Met^{11} HN	Leu^{10} HA	3.52	3.45	0.15
Met^{11} HN	Met^{11} HA	2.49	2.52	0.13
MePhe^8 CH_3	Asp^6 HA	< 5	5.37	
MePhe^8 CH_3	Phe^7 HN	< 4	5.36	
Gly^9 HN	Asp^6 HB1	< 5	3.66	
Leu^{10} HB1	Phe^7 HB1	< 6	4.17	
Leu^{10} HB1	Phe^7 CG	< 6	6.17	
Met^{11} HN	Asp^6 HB1	< 5	4.91	
Met^{11} HN	Phe^7 HB1	< 5	5.03	
Met^{11} HN	Met amide HT1	< 5	3.39	
Met^{11} HA	Met amide HT2	< 5	3.53	
Met amide HT1	Asp^6 HB1	< 5	5.31	
Met amide HT2	Gly^9 HA2	< 5	4.83	

[a] Distance violations are expressed as number of standard deviations (SD). SD was 0.2 Å for distances < 2.5 Å (strong NOEs) and 0.45 Å for longer distances. Violations expressed in Å can be obtained by simple multiplication by SD. Violations less than 1 SD are statistically acceptable.

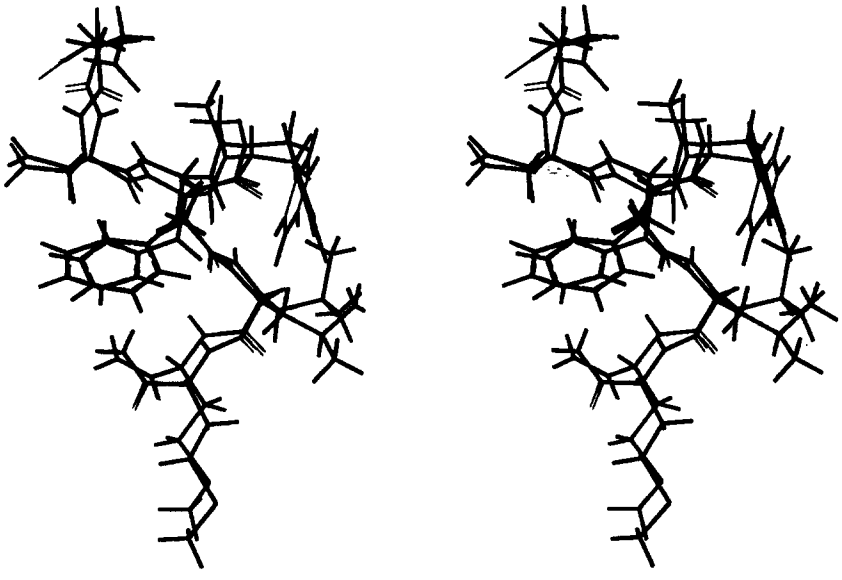

Fig. 5. Comparison of a FILMAN conformation (senk1) before and after energy minimization.

conformation. The few data collected on the cis isomer were insufficient to obtain some insight into its conformational behavior.

The trans isomer gave rise to a large number of TRNOEs. It was shown by inspection of the time dependence of TRNOE cross-peak volumes that spin-diffusion is not important in our experimental conditions, even at relatively long (300 ms) mixing times. This is due to the fact that the effective mixing time in this experiment is the product of the experimental τ_m and the fraction

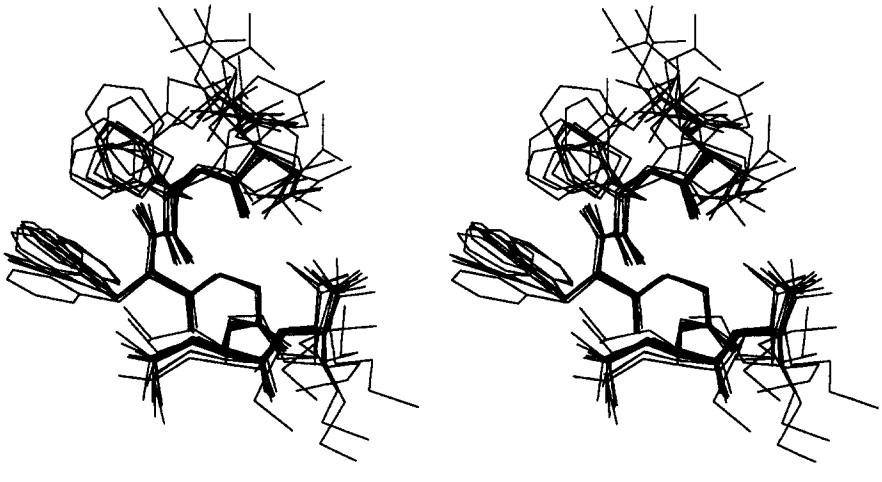

Fig. 6. Superposition of 10 membrane-bound conformations of the senktide trans isomer. The best fit was taken over all backbone atoms.

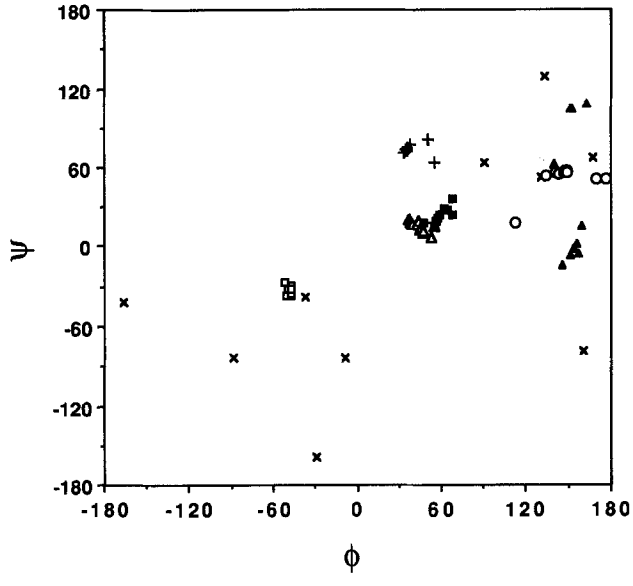

Fig. 7. Ramachandran diagram of the ϕ and ψ torsion angles of the 10 FILMAN structures of the senktide trans isomer. × = Succ^0; ○ = Asp^6; + = Phe^7; △ = MePhe^8; ■ = Gly^9; □ = Leu^{10}; ▲ = Met^{11}.

bound (which can be estimated to be in the range of 10^{-3} to 10^{-2}). Similar backbone conformations could be obtained with either a full set of 99 upper-bound constraints or a limited set containing mainly backbone–to–backbone exact distances. A superposition of the 10 selected conformations of the trans isomer obtained in the first FILMAN runs, achieved with the optimum fit procedure of the SYBYL program, is shown in Fig. 6. The backbone is seen to be well constrained, as confirmed by the spread in the values of the backbone dihedral angles of these structures (Table 3). A word of caution is in order here: the low standard deviations obtained on the values of ϕ and ψ over the 10 selected structures (STD1, Table 3) do not provide an estimate of the quality of the refined structures according to the quality of the input data; a better estimate of the structure's accuracy, in the least-square sense, is directly given by FILMAN (Koehl et al., 1992). The corresponding values in the case of senk1 are reported in Table 3 (STD2) and indicate that most backbone angle values are reliable within +/−20°.

The constraints derived from these TRNOEs reveal that the four central hydrophobic amino acids adopt a well-defined conformation, with an average distance error of 0.1 Å, whereas the N- and C-termini are more mobile. This can be rationalized in terms of the interaction with the membrane: the interaction is hydrophobic in its nature and imposes one conformation on the central amino acid (backbone and side chains). The aspartic acid is mobile and this is reasonable considering that succinate and aspartate side chains resemble each other and may have identical interactions at the bilayer interface; one can expect that interchanging the chains leads to highly similar interactions with the membrane interface.

Inspection of the ϕ and ψ angles in Table 3 shows that all pairs except the one of Leu^{10} are situated in an energetically disfavored region of a standard Ramachandran diagram (positive ϕ and ψ values) as shown in Fig. 7. On the other hand, the total energy of the molecule after energy minimization was found to be quite low, which does indicate a stable conformer in spite of this

specific backbone orientation. The occurrence of the positive backbone dihedral angles is certainly due to the presence of the N-methylated phenylalanine. In fact, the energetically favored angle spaces of residues preceding or following N-methylated peptide bonds are different from those of normal amino acids (Manavalan and Momany, 1980; Iijima et al., 1987). N-methylated peptide bonds have the tendency to limit the conformational space for the classical α-helix because of the contact between the amide protons of the first and the N-methyl protons of the following residue. Moreover, in the senktide sequence, the N-methylated phenylalanine is followed by a glycine, i.e. a residue for which positive ϕ and ψ angles are common. The FILMAN structures indicate hydrogen bonding from Asp^6 CO to Gly^9 H_N and from Phe^7 CO to Leu^{10} H_N. All the bulky hydrophobic side chains are situated very close to each other, as demonstrated by numerous TRNOESY cross peaks between them.

Side chains of such a short peptide are expected to be less ordered than the backbone, even in the membrane-bound state which certainly retains liquid-like characteristics. Interestingly, side chains of $MePhe^8$ and Leu^{10} were found to be well restrained (Fig. 6). Some ambiguity arose about the orientation of the Phe^7 side chain. In most cases, the χ^1 value was −115°, but for a few structures, this angle was found to be 20°. The localization of the Phe^7 side chain is determined by the TRNOEs from the aromatic protons to the methyl group of the Leu^{10} side chain, its own amide proton, and by a weak TRNOE to the overlapping protons at the resonance frequency of the Asp^6 side-chain protons. The TRNOE with the Leu^{10} side chain is in favor of the negative χ^1 angle, but cannot account for the TRNOE observed to the Asp^6 or $Succ^0$ methylene protons. On the other hand, the positive χ^1 angle was not consistent with the close contact to the Leu^{10} methyl protons. This is in favor of a rapid reorientation of the Phe^7 side chain when interacting with the membrane.

Until now, only little structural information on NK-3 agonists has been reported in the literature. NMR investigations of neurokinin B and one of its analogs [$pGlu^6$, N-$MePhe^8$]SP(6–11) performed in DMSO, resulted in structures which were also characterized by a very close contact of the C- and the N-terminal (Levian-Teitelbaum et al., 1989; Loeuillet et al., 1989). However, these structures were not given with the same precision as ours. In addition, senktide has been studied by NMR in methanol, but this structure was clearly different from ours (Sumner and Ferretti, 1989).

As pointed out earlier, the membrane could play an important role in the binding of neuropeptides to their receptor molecule. In order to apply the membrane-compartment theory to the tachykinin system, Schwyzer estimated various parameters related to the membrane interaction of different tachykinins and their analogs (Schwyzer, 1987). These calculations were performed in analogy to those already used for the estimation of the membrane-bound structure and orientation of substance P (Schwyzer et al., 1986). While assuming that the interaction of the peptide with the membrane resulted in an α-helical conformation, a hypothetic dissociation constant K_d was calculated, taking into account hydrophobic or electrostatic interactions with the membrane. In the case of senktide, both constants were found to be very low (16 M from the hydrophobic, 22.5 M from the electrostatic interaction with a Gouy–Chapman surface potential set to −40 mV) and are in contradiction with the pronounced membrane interaction of senktide observed in our TRNOE experiments. This can be explained by the fact that the membrane-bound conformation of trans senktide is not α-helical; our conformation having hydrophobic side-chain parallels interacts with the bilayer mainly through hydrophobic forces.

Senktide has been found to interact with the NK-3 receptor in the nanomolar concentration range (Laufer et al., 1986; Wormser et al., 1986). It becomes clear that in this case the very high

affinity cannot be explained by a simple accumulation of the peptide at the surface of the membrane due to electrostatic interactions. In the case of the positively charged substance P, the apparent binding constant (10^6 M^{-1}), including the accumulation of the peptide near the negatively charged bilayer, was two to three orders of magnitude higher than the intrinsic binding constant, determined only by the hydrophobic interactions (Seelig and Macdonald, 1989). Therefore, the role of the membrane interaction for the binding of senktide to its receptor should essentially be a structural one, for example by the induction of a conformation which would favor the immediate and efficient binding to the receptor. This could be the observed turn structure, characterized by the proximity of the hydrophobic chains. Requirement of a folded C-terminal has been deduced from pharmacological investigations with conformationally constrained analogs, bearing a lactam ring in position 9 of the substance P sequence (Cascieri et al., 1986). On the other hand, the possibility cannot be excluded that repulsive forces between the membrane surface and the peptide would guide the latter to the active site, situated at the outside of the membrane. In addition, receptor–subtype specificity could be obtained by preventing the peptide to get close to the binding sites of the NK-1 and NK-2 receptors. This is in good agreement with the membrane-compartment theory proposed by Schwyzer (Schwyzer, 1987). In addition, nothing is currently known about the possible role of the cis isomer. Resulting from our TRNOE investigation, the cis isomer shows a lower affinity for the membrane than does the trans isomer, which might be due to its inability to create sufficient hydrophobic interactions due to a different backbone conformation.

The membrane conformation of senktide defined in our study may contribute to a further elucidation of the specific peptide–receptor interaction, as it may guide the design of new analogs, mimicking the membrane-bound conformation. Results of such investigations will be very interesting, as they could help to evaluate the structural role of the membrane interaction, like in the case of senktide where accumulation on the membrane surface was excluded. Finally, our demonstration of the different interaction of cis and trans isomers with lipid membranes provides new guidelines for understanding the influence of the Phe^8 N-methylation on the affinity and receptor subtype selectivity of senktide. Two possible alternatives are now clear: either the cis isomer is the active one and it binds directly to the receptor or it is the trans isomer which interacts with the receptor in multistep kinetics involving membrane-bound stages.

Having demonstrated that the transferred-NOE approach in the presence of perdeuterated liposomes can be applied successfully to the tachykinin family, we are now working on other peptides specific for NK-1 and NK-2 receptors in order to correlate receptor subtype specificity and membrane interactions.

ACKNOWLEDGEMENTS

We thank Prof. J.F. Lefèvre for access to the Bruker 500 MHz spectrometer, Elf Aquitaine for financial support to B. Bersch, and Dr W. Dellsberger and Dr J.M. Bernassau for their help and encouragement.

REFERENCES

Banks, K.M., Hare, D.R. and Reid, B.R. (1989) *Biochemistry*, **28**, 6996–7010.

Bax, A. and Davis, D.G. (1985a) *J. Magn. Reson.*, **63**, 207–213.

Bax, A. and Davis, D.G. (1985b) *J. Magn. Reson.*, **65**, 355–360.

Behling, R.W. and Jelinski, L.W. (1990) *Biochem. Pharmacol.*, **40**, 49–54.

Bersch, B., Stark, J.P., Milon, A., Nakatani, Y. and Ourisson, G. (1993) *Bull. Soc. Chim. Fr.*, in press.

Billeter, M., Braun, W. and Wüthrich, K. (1982) *J. Mol. Biol.*, **155**, 321–346.

Bothner-By, A.A., Stephens, R.L., Lee, J., Warren, C.D. and Jeanloz, R.W. (1984) *J. Am. Chem. Soc.*, **106**, 811–813.

Braunschweiler, L., Bodenhausen, G. and Ernst, R.R. (1983) *Mol. Phys.*, **48**, 535–560.

Braunschweiler, L. and Ernst, R.R. (1983) *J. Magn. Reson.*, **53**, 521–528.

Buck, S.H., Van Giersbergen, P.L.M. and Burcher, E. (1991) *Neurochem. Int.*, **18**, 167–170.

Campbell, A.P. and Sykes, B.D. (1991) *J. Magn. Reson.*, **93**, 77–92.

Cascieri, M.A., Chicchi, G.G., Freidinger, R.M., Dylion Colton, C., Perlow, D.S., Williams, B., Curtis, N.R., McKnight, A.T., Maguire, J.J., Veber, D.F. and Liang, T. (1986) *Mol. Pharmacol.*, **29**, 34–38.

Chassaing, G., Convert, O. and Lavielle, S. (1986) *Eur. J. Biochem.*, **154**, 77–85.

Clore, G.M. and Gronenborn, A.M. (1983) *J. Magn. Reson.*, **53**, 423–442.

Dam, T.V., Escher, E. and Quirion, R. (1990) *Brain Res.*, **506**, 175–179.

Drapeau, G., D'Orléans-Juste, P., Dion, S., Rhaleb, N.E. and Regoli, D. (1987) *Eur. J. Pharmacol.*, **136**, 401–403.

Gasteiger, J. and Marsili, M. (1980) *Tetrahedron*, **36**, 3219–3228.

Guard, S. and Watson, S.P. (1991) *Neurochem. Int.*, **18**, 149–165.

Guard, S., Watson, S.P., Maggio, J.E., Too, H.P. and Watling, K.J. (1990) *Brit. J. Pharmacol.*, **99**, 767–773.

Hruby, V.J. (1982) *Life Sci.*, **31**, 189–199.

Iijima, H., Dunbar, J.B. and Marshall, G.R. (1987) *Protein Struct. Funct. Genet.*, **2**, 330–339.

Jeener, J., Meier, B.H., Bachmann, P. and Ernst, R.R. (1979) *J. Chem. Phys.*, **71**, 4546–4553.

Jelicks, L.A., Broido, M.S., Becker, J.M. and Naider, F.R. (1989) *Biochemistry*, **28**, 4233–4240.

Kingsley, P.B. and Feigenson, G.W. (1979) *Chem. Phys. Lipids*, **24**, 135–147.

Koehl, P., Lefèvre, J.F. and Jardetzky, O. (1992) *J. Mol. Biol.*, **223**, 299–315.

Laufer, R., Gilon, C., Chorev, M. and Selinger, Z. (1986) *J. Biol. Chem.*, **261**, 10257–10263.

Lavielle, S., Chassaing, G., Ploux, O., Loeuillet, D., Besseyre, J., Julien, S., Marquet, A., Convert, O., Beaujouan, J.C., Torrens, Y., Bergström, L., Saffroy, M. and Glowinski, J. (1988) *Biochem. Pharmacol.*, **37**, 41–49.

Levian-Teitelbaum, D., Kolodny, N., Chorev, M., Selinger, Z. and Gilon, C. (1989) *Biopolymers*, **28**, 51–64.

Lippens, G.M., Cerf, C. and Hallenga, K. (1992) *J. Magn. Reson.*, **99**, 268–281.

Loeuillet, D., Convert, O., Lavielle, S. and Chassaing, G. (1989) *Int. J. Pept. Protein Res.*, **33**, 171–180.

London, R.E., Perlman, M.E. and Davis, D.G. (1992) *J. Magn. Reson.*, **97**, 79–98.

Macura, S. and Ernst, R.R. (1980) *Mol. Phys.*, **41**, 95–117.

Maggio, J.E. (1988) *Annu. Rev. Neurosci.*, **11**, 13–28.

Manavalan, P. and Momany, F.A. (1980) *Biopolymers*, **19**, 1943–1973.

Mareci, T.H. and Freeman, R. (1983) *J. Magn. Reson.*, **51**, 531–535.

Marion, D. and Wüthrich, K. (1983) *Biochem. Biophys. Res. Commun.*, **113**, 967–974.

McLachlan, A.D. (1979) *J. Mol. Biol.*, **128**, 49–79.

Milon, A., Miyazawa, T. and Higashijima, T. (1990) *Biochemistry*, **29**, 65–75.

Nakanishi, S. (1991) *Annu. Rev. Neurosci.*, **14**, 123–136.

Plateau, P. and Guéron, M. (1982) *J. Am. Chem. Soc.*, **104**, 7310–7311.

Rance, M., Sørensen, O.W., Bodenhausen, G., Wagner, G., Ernst, R.R. and Wüthrich, K. (1983) *Biochem. Biophys. Res. Commun.*, **117**, 479–485.

Regoli, D., Dion, S., Rhaleb, N.E., Rouissi, N., Tousignant, C., Jukic, D., D'Orleans-Juste, P. and Drapeau, G. (1989) *Biopolymers*, **28**, 81–90.

Regoli, D., Drapeau, G., Dion, S. and Couture, R. (1988) *Trends Pharmacol. Sci.*, **9**, 290–295.

Sargent, D.F., Bean, J.W. and Schwyzer, R. (1988) *Biophys. Chem.*, **31**, 183–193.

Sargent, D.F., Bean, J.W. and Schwyzer, R. (1989) *Biophys. Chem.*, **34**, 103–114.

Sargent, D.F. and Schwyzer, R. (1986) *Proc. Natl. Acad. Sci. USA*, **83**, 5774–5778.

Saulitis, J. and Liepins, E. (1990) *J. Magn. Reson.*, **87**, 80–91.
Schwyzer, R. (1987) *EMBO J.*, **6**, 2255–2259.
Schwyzer, R. (1991) *Biopolymers*, **31**, 785–792.
Schwyzer, R., Erne, D. and Rolka, K. (1986) *Helv. Chim. Acta*, **69**, 1789–1797.
Seelig, A. and Macdonald, P.M. (1989) *Biochemistry*, **28**, 2490–2496.
Shaka, A.J. and Freeman, R. (1983) *J. Magn. Reson.*, **51**, 169–173.
Sumner, S.C.J. and Ferretti, J.A. (1989) *FEBS Lett.*, **253**, 117–120.
Wakamatsu, K., Okada, A., Suzuki, M., Higashijima, T., Masui, Y., Sakakibara, S. and Miyazawa, T. (1986) *Eur. J. Biochem.*, **154**, 607–615.
Wakamatsu, K., Okada, A., Suzuki, M., Higashijima, T., Sakakibara, S. and Miyazawa, T. (1987) *Eur. J. Biochem.*, **163**, 331–338.
Williamson, M.P. and Neuhaus, D. (1987) *J. Magn. Reson.*, **72**, 449–457.
Wormser, U., Laufer, R., Hart, Y., Chorev, M., Gilon, C. and Selinger, Z. (1986) *EMBO J.*, **5**, 2805–2808.
Wüthrich, K. (1986) *NMR of Proteins and Nucleic Acids*, Wiley, New York.
Wüthrich, K., Billeter, M. and Braun, W. (1983) *J. Mol. Biol.*, **169**, 949–961.